TESTING AND REFURBISHMENT OF SCINTILLATORS FOR JEFFERSON LABORATORY

by

Juan Lukas Rodriguez

A Senior Thesis Submitted to the Faculty of the Department of Physics
Old Dominion University in Partial Fulfillment of the
Requirement for the Degree of

BACHELOR OF SCIENCE

PHYSICS

OLD DOMINION UNIVERSITY

August 2017

Approved by:

_____
Dr. Lawrence Weinstein
(Advisor)

_____
Dr. Mark Havey

_____
Dr. Gail Dodge

ABSTRACT

Testing and Refurbishment of Scintillators for Jefferson Laboratory

Juan Lukas Rodriguez
Old Dominion University, August 2017
Advisor: Dr. Lawrence Weinstein

This thesis describes the testing and refurbishment of scintillator detectors for the Large Acceptance Detector at Jefferson Laboratory. The testing was done at various voltages and the resultant data was analyzed for efficiency, pulse height, attenuation length and time resolution. This determined optimal voltage for each photomultiplier tube. This thesis describes the testing procedures, data acquisition, and output analysis necessary for evaluating the continued usefulness of the scintillator detectors with appropriate refurbishment.

This thesis is dedicated to Juana Rodriguez

ACKNOWLEDGMENTS

I would like to thank my thesis advisor and mentor, Dr. Lawrence Weinstein, for his guidance, support, and patience as I struggled to learn the workings of the high bay lab, gather and analyze data, and prepare this thesis over the past several semesters. Overcoming these challenges took me longer than expected and I am truly grateful for Dr. Weinstein's continued support.

I would also like to thank my thesis examination committee, Dr. Mark Havey and Dr. Gail Dodge.

My appreciation for assistance in the High Bay Lab goes to Katheryne McMahan and Tom Hartlove. Their help with instrument and equipment setups, data acquisition, and overall reinforcement was invaluable.

Finally, I would like to acknowledge the support and encouragement of my friends and family. Without their consistent patience, I would not have completed this final requirement for my degree.

TABLE OF CONTENTS

Page

LIST OF TABLES

LIST OF FIGURES

INTRODUCTION

In partnership with the US Department of Energy's Thomas Jefferson National Accelerator Facility (JLab, Figure 1), physics students at Old Dominion University have been testing and refurbishing particle detectors in the school's Nuclear and Particle Physics High Bay Laboratory (Figure 2). The 3.9 to 4.5 meter long particle detectors, which are used in research projects to study the nuclei of atoms, are shipped from JLab in Newport News to ODU's High Bay Lab. Testing determines if the detectors show tiny flashes of light when charged particles or radiation pass through them.[1]

Specifically, my task was to refurbish scintillator detectors from JLab's Hall B by testing, measuring and analyzing various characteristics. The scintillators were individually tested at various voltages. The data was then analyzed for efficiency, pulse height, attenuation, and time resolution. After looking at the data, the optimal voltages were recorded. If the pulse height was too low or efficiency was not high enough, then the Photo Multiplier Tube (PMT) was removed and replaced.

Figure 1 Aerial view of Jefferson Laboratory

Photo credit: Jefferson Lab website flicker photos

Figure 2 High Bay Lab at ODU

Photo credit: Juan Lukas Rodriguez

[1] Noel Saunders, *JLab Particle Detectors, Used in Nuclear Research, Arrive for Refurbishment*. June 2017. https://www.odu.edu/news/2017/6/particle_detector#.

CHAPTER 1

SCINTILLATORS

1.1. What is a Scintillator?

Scintillator detectors are one of the most popular types of particle detectors used in particle and nuclear physics. They are able to detect incoming charged particles and radiation by producing a "flash of light," also known as scintillating, and creating an electronic signal for scientists to read using a photomultiplier tube (PMT). Scintillators are made of certain types of luminescent materials that exhibit the property of scintillation. Scintillation occurs when a high energy charged particle passes through a scintillant or a high energy photon is absorbed in a scintillant. Energy is then deposited in the scintillant and excites or ionizes electrons. The electrons de-excite or recombine, emitting light – also known as scintillating.

1.2. Types of Scintillators

There are many different types of luminescent materials, but only a few are useful as scintillator detectors. In general, to be useful as scintillator, the luminescent material should exhibit high efficiency in converting the particle's deposited energy into visible light. The time it takes the atoms of the material to absorb and reemit energy should be short (about 10 nano-seconds). This measure is also known as the decay constant. The material should be transparent in order for the reemitted light to travel through the scintillator. In addition, the emission of light should also be in the correct spectral range. There are six different types of scintillator materials: organic crystals, organic liquids,

plastic, inorganic crystals, gases, and glasses. Plastic scintillators, which are the most common, were used in this project (Figure 3).

Figure 3 Plastic scintillator

Photo credit: Juan Lukas Rodriguez

1.3. Scintillator and Photomultiplier Tube (PMT) Mechanics

There are four main parts to the scintillator detector: the scintillating material, the light guide, the photomultiplier tube (PMT), and the voltage divider. When charged particles enter the scintillator material, the atoms of the material get excited and scintillate. This flash of light then travels through the scintillator to the light guide attached on the end. The light guide guides the light to hit the photocathode on the PMT.

The PMT is an electron tube that converts light into a measurable electric current. It consists of a photocathode, dynodes, and anodes. At the top of the PMT is the photocathode, receiving light from the light guide. Photons free electrons from their atoms in the photocathode via the photoelectric effect. These electrons are accelerated and focused to hit the first dynode held at potential difference. At the dynode, the electrons cause secondary emission of more electrons. As the electrons hit each dynode more electrons are emitted via secondary emission. This amplifies the electrical signal more and more as it goes through the series of dynodes. At the end, the anode collects the electrons and produces a readable signal.[2] Figure 4 is a diagram of the PMT.

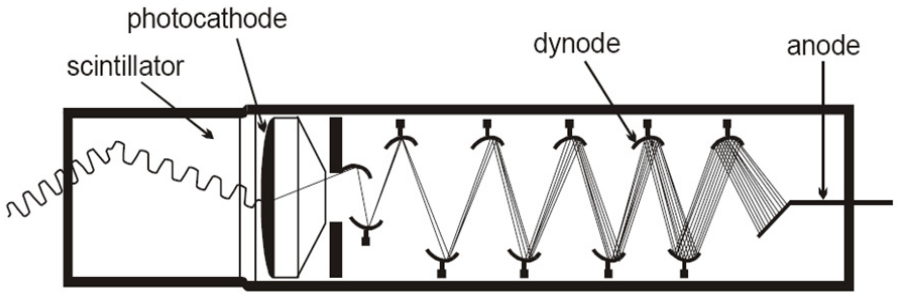

Figure 4 Diagram of Photomultiplier Tube (PMT)

Illustration credited to Lab-Training.com

[2] W.R. Leo, *Techniques for Nuclear and Particle Physics Experiments*, p 177,

CHAPTER 2

LAB SETUP

2.1. Jefferson Lab Scintillator Background

The scintillators that needed refurbishment were 136 CLAS6 TOF (time of flight) scintillators. Eleven scintillator detectors from JLab arrived at ODU on a frame in May 2016. This was the fourth frame of scintillators JLab sent to Old Dominion for refurbishing.

The scintillators were in constant use for over twenty years at JLab (Figure 5). The scintillator detectors were part of the time of flight system in the CEBAF Large Acceptance Spectrometer in JLab's Hall B. They will be reused in the EMC-SRC experiment in Hall C. [3]

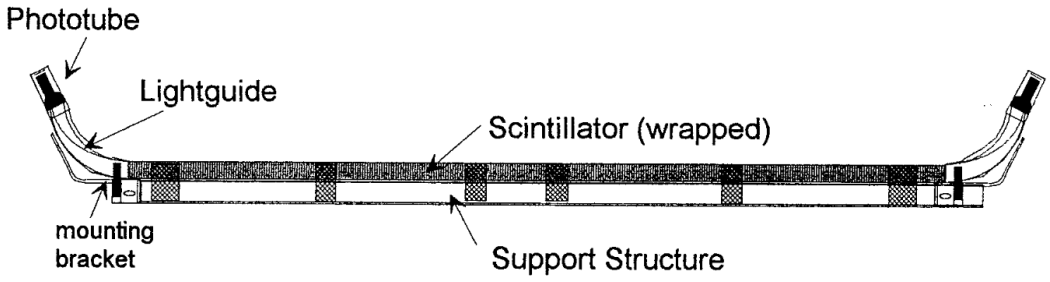

Figure 5 Diagram of a large angle scintillator detector

This illustration was found in the UNH Nuclear Instrument Lab's 1996 CEBAF Time of Flight Detectors Final Project Report.[4] This is the type of detector in Hall B of JLab.

[3] E.S. Smith, *The Time-of-Flight System for CLAS*. NH Elsevier: Nuclear Instruments and Methods in Physics Research A 432 (1999) 265-298.
[4] Korac J. McArthur, UNH Nuclear Instrumentation Lab CEBAF Time of Flight Detectors Final Project Report, July 17, 1996. Jefferson Laboratory website library.

2.2. Jefferson Lab Scintillator Structure

The scintillators (model BC-408) are made of polyvinyl toluene, doped with the aromatic hydrocarbon anthracene. They are wrapped with two layers of aluminum foil and one layer of thick, black carbon doped mylar. Each detector has dimensions of about 4 meters long, 22.5 centimeters wide, and 5 centimeters thick.[5] A light guide is attached to the end of the scintillator (Figure 6). The light guide is acrylic plastic, also known as polymethylmethacrylate (PMMA), which is commonly used for plastic scintillators because it is optically clear and has good mechanical properties. The scintillators have a PMT and voltage divider on each end.

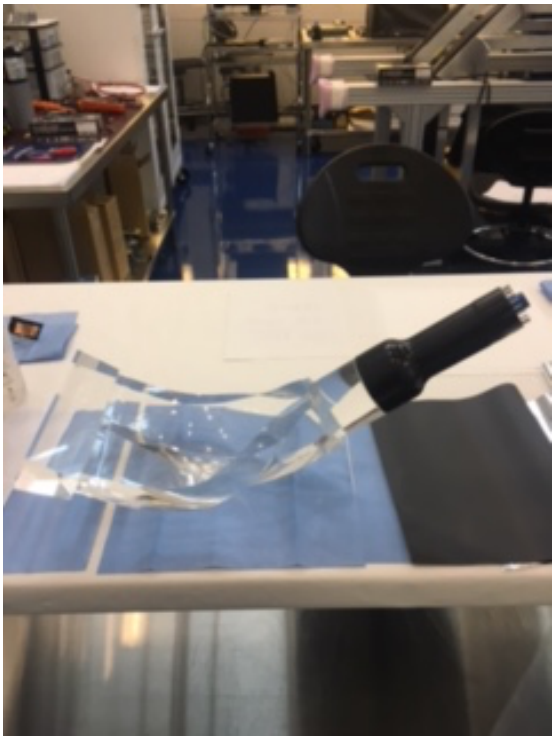

Figure 6 Photomultiplier Tube (PMT) with light guide

Photo credit: Juan Lukas Rodriguez

[5] Korac J. McArthur, UNH Nuclear Instrumentation Lab CEBAF Time of Flight Detectors Final Project Report, July 17, 1996. Jefferson Laboratory website library.

The PMT slides into a cylindrical barrel that has an inner mu metal magnetic shield. The shield prevents external magnetic fields from affecting the current in the PMT. With the PMT inside, the barrel is attached to the end of the light guide. At the end of the PMT, a voltage divider is attached to the pins. The voltage divider connects the pins at the end of the PMT to the different voltages. The voltage divider consists of a high voltage terminal, an anode terminal, and a dynode terminal.

2.3. Initial Testing

These scintillators are over 20 years old and require some initial testing for bad PMTs. We first connected the PMT's anode output to the oscilloscope via lemo-cable and connected the PMT to the high voltage, to find a readable signal. I increased the voltage slowly, until I saw a good signal on the oscilloscope. A good signal has a rapid rise, about negative 400-1000 mV in amplitude and 20-30 nano seconds long. Once we observed a good readable signal, we performed a counting test.

When there are no good signals, or too many, the voltage divider might be not grounded properly or there might be a light leak. To ground the voltage divider, the plastic barrel was removed. The barrel is covered with aluminum on the outside with black electrical tape placed over the aluminum. The voltage divider must be properly grounded on both the outside and inside of the barrel. Copper tape must be touching the outside of the barrel where the aluminum is placed and on the bottom metal part of the voltage divider. Inside of the barrel, the wire is secured with copper tape to the mu-metal magnetic shield.

To conduct the counting test, I attached the PMT anode output to a discriminator and then to a counting module via lemo cables. The discriminator changes the analog signal to a digital signal. The threshold of the discriminator is set at -60mV, meaning that only signals reaching an amplitude of at least -60mV create digital signals. The discriminated digital signal is sent to the Counting Module which counts the number of signals for a set time of 10 seconds. Each PMT was tested at voltages ranging from 1600 V to 2400 V until they reached at least 5000 counts. If it failed to count to 5000 with 2400 V, then the voltage divider (Figure 7) was further tested to see if it was malfunctioning.

The second thing measured was the coincidence count number of the two PMTs on each scintillator. This time, the PMTs on each end of a scintillator were connected to a discriminator and then the two digital signals were connected to an AND unit. The AND unit sends a signal through only if both PMTs were able to produce a sufficient signal for that event. The required number of counts for this test was 1500. Generally, the longer length scintillators had more counts due to the greater surface area of the scintillator.

If the PMTs did not meet the required number of counts by 2400 V, the voltage dividers were detached from the scintillator and connected to a voltage supply at 2000 V. Using a fluke multi meter, the voltage on each pin was measured and recorded. If the voltage difference between each pin was within 10% of their accepted value, then the voltage divider was satisfactory. If the voltage difference between each pin fell outside 10% of the expected difference, then the voltage divider was replaced. If the voltage

divider was satisfactory, the PMT was deemed bad and replaced. Replacement is discussed in Chapter 3.

Figure 7 Voltage Divider

Photo credit: Juan Lukas Rodriguez

2.4. Rack Testing Setup

Once the scintillators were functioning properly, we measured their efficiency, time resolution, pulse height (ADC peak), and attenuation length. To start off, three scintillators were set up on a vertical rack (Figure 8). The scintillators were stacked vertically with equal distances between them. The middle scintillator is the one that was tested and the top and bottom scintillators served as the triggers for the data acquisition. The data acquisition will read out the event only if both top and bottom scintillators registered the particle. An event happens when negatively charged muons from cosmic rays penetrate the top and bottom scintillators. Muons are negatively charged particles

heavier than electrons. Muons penetrating both the top and bottom scintillators will almost surely hit the middle one. Thus, this setup helps determine a true event.

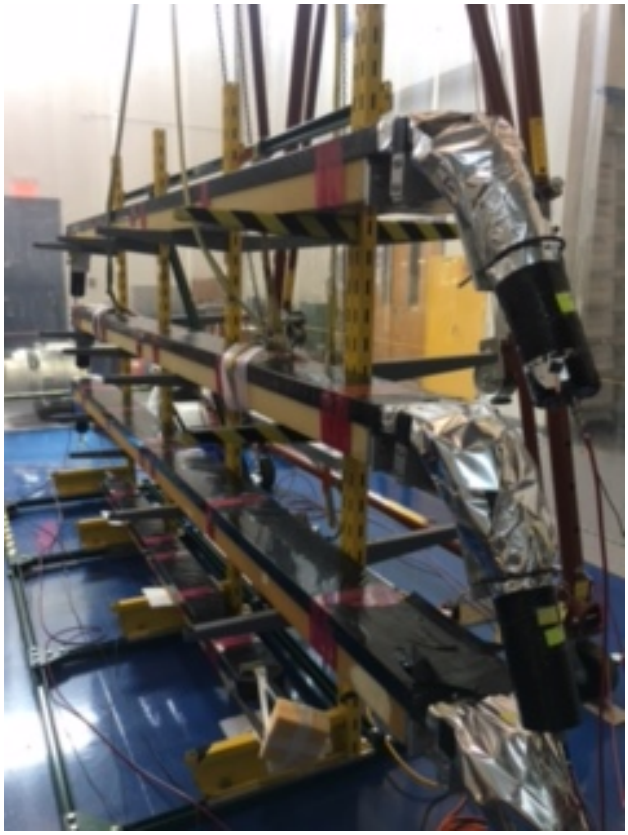

Figure 8 Scintillators on a vertical rack in ODU's High Bay Lab

Photo credit: Juan Lukas Rodriguez

The rack testing setup includes three electronic logical structures: one each for the Trigger, the time to digital converter (TDC) module, and the analog to digital converter (ADC) module.

For the trigger logic structure, there are four input signals: the two top and two bottom PMT signals. All four signals are connected to separate fanout inputs. Each fanout will create two output signals. One output signal will go to a discriminator module, which will turn the analog signal into a digital signal (threshold = -60mV). That

signal will go to the four-fold logic unit. The signal from the bottom right is delayed by 31ns so it will always determine the trigger time. The four-fold logic unit will only produce an output signal if all four signals are true simultaneously; they all must wait for the bottom right PMTs 31 ns delay to trigger the start. One output of the four-fold discriminator will go straight to the TDC module's start trigger input. This will tell the TDC to start counting. The other signal will go through a second discriminator to create a longer output pulse. That longer signal will be sent to the ADC gate input.

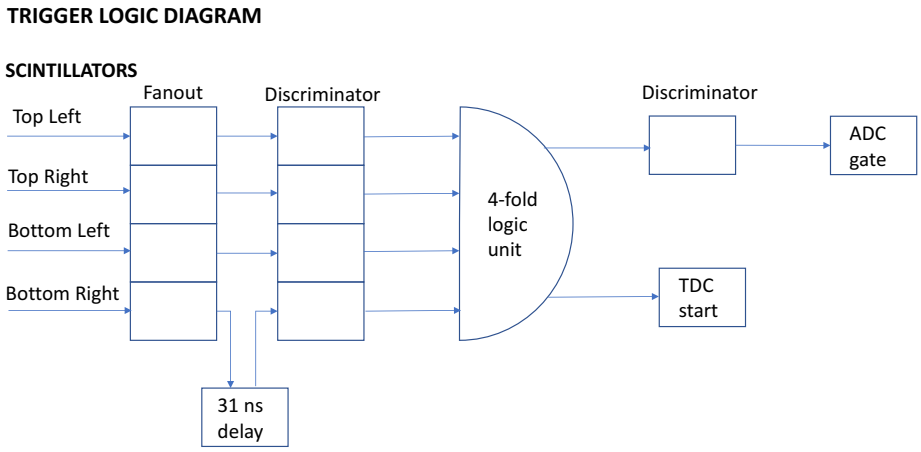

Figure 9 Trigger Logic Diagram

Illustrates both top and bottom scintillators on the test rack

The TDC module is a device that measures the time between two signals by measuring the discharge of a capacitor. The measure of charge is in units called channels. Each channel represents 50 pico seconds. Information from the TDC module is used to determine the time resolution and efficiency of the scintillator. Like the trigger logic setup, there is a similar logic setup for TDC data acquisition.

All six signals from each PMT go through the fanout and then to the discriminator, which is set at negative 60 mV threshold. The signals then all go through a 119 nano-second delay. This allows the signals to arrive after the TDC start signal. After the delay, the signals go to the inputs of the TDC module. The inputs are labeled from channel 0--5.

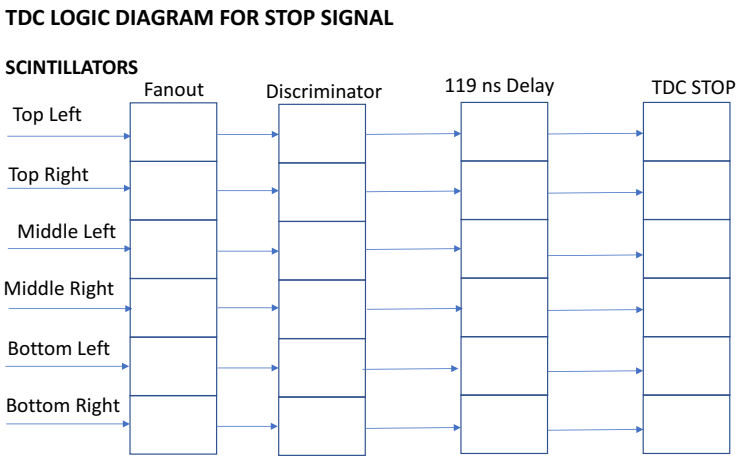

Figure 10 Time to Digital Converter (TDC) Logic Diagram

Illustrates top, middle, and bottom scintillators on the test rack

The ADC module measures the charge of the signal produced by the PMT. The ADC integrates the incoming signal and converts it to digital values called channels. We used this device to measure pulse height and attenuation length. The ADC logic structure is the same as the TDC logic structure, but this time all 6 signals from the PMTs skip the discriminator and go straight to the 119 ns delay. The analog then goes to the ADC module.

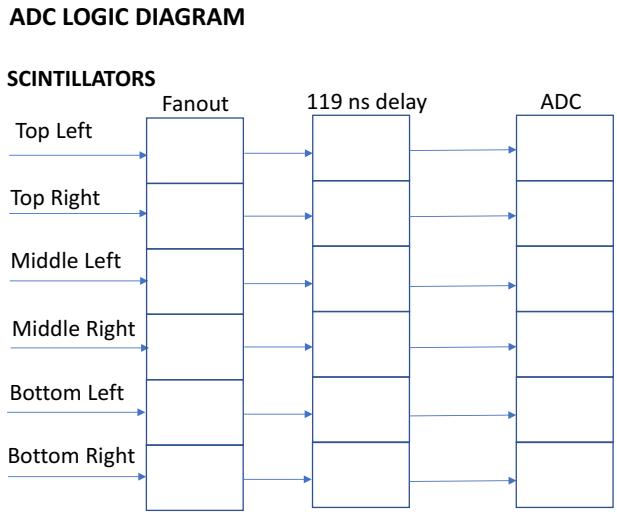

Figure 11 Analog to Digital Converter (ADC) Logic Diagram

Illustrates top, middle, and bottom scintillators on the test rack

2.5. Data Acquisition Using CAMAC Crate

Once the electronic logic sends signals to the ADC and TDC, the data acquisition can take place using a CC-USB interface with a computer. The CC-USB is a CAMAC controller that has a high speed USB interface. Either the ADC or TDC is connected via lemo cable to the CC-USB. The CC-USB is connected with a USB into the computer.

We used a computer program called "XXUSBWin" to read out data from CAMAC. To run the program from the XXUSBWin, I first created a Primary Command Stack. The Primary Command Stack is a sequence of commands that are executed from a trigger. In this case, the ADC gate and TDC start are the trigger. When the ADC and TDC are finished registering an event, the commands are executed. Each command consists of four hexadecimal numbers. These numbers represent the TDC or ADC

location or slot number on the crate “N”, the address corresponding to each channel in the TDC and ADC “A”, and the actual command that reads the data “F”.

Once the stack is built, it is loaded on the DAQ section in the XXUSBWin. Before XXUSBWin runs, the start delay must be at least 10 micro seconds, to provide time for all the signals to be processed. In addition, the Output File Format must be decimal and the Use Init Stack box must be checked. Once complete, the DAQ may start and run. Usually the run was 5 minutes for each voltage. Once the operating voltage was found, a three-hour run was conducted.

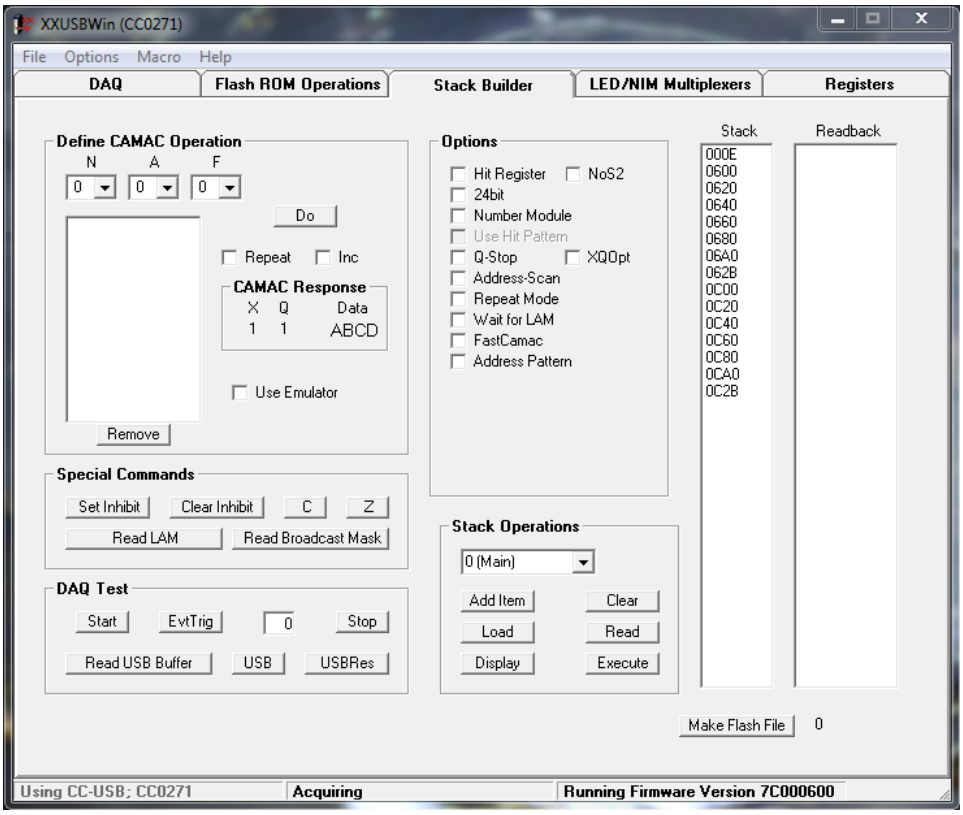

Figure 12 The XXUSB-WIN Stack builder panel

Table 1 List of Stack Commands for Data Acquisition

N	A	F	Description of Command
0	0	23	Resets Entire Module
3	0	0	Reads information from channel 0 of the TDC
3	1	0	Reads information from channel 0 of the TDC
3	2	0	Reads information from channel 0 of the TDC
3	3	0	Reads information from channel 0 of the TDC
3	4	0	Reads information from channel 0 of the TDC
3	5	0	Reads information from channel 0 of the TDC
3	1	11	Resets the hit register
6	0	0	Reads information from channel 0 of the ADC
6	1	0	Reads information from channel 0 of the ADC
6	2	0	Reads information from channel 0 of the ADC
6	3	0	Reads information from channel 0 of the ADC
6	4	0	Reads information from channel 0 of the ADC
6	5	0	Reads information from channel 0 of the ADC
6	0	11	Resets the hit register

CHAPTER 3

REMOVING AND REPLACING PMTs

3.1. Barrel and PMT Removal

Removal of the PMT was not an easy task. I first removed the barrel from the PMT by unscrewing the U bolt and then removed the electrical tape that was attached to the aluminum around the barrel. I then folded back the aluminum foil. By carefully tapping on a thin blade with a hammer near where the light guide and the PMT meet (see Figure 13), an air pocket formed between the light guide and PMT. Once the air pocket became big enough, a clean removal of the PMT was possible. Sometimes though, the glass on the PMT would crack leaving chunks of glass stuck to the light guide. I used isopropyl alcohol to remove the glass from the light guide. Isopropyl alcohol dissolves the glue and makes it easier to remove the glass.

Figure 13 Blade placement for removing PMT

Photo credit: Juan Lukas Rodriguez

3.2. Polishing and Cementing

After I removed the glass from the light guide, I polished the light guide. Using water and sand paper at different number grits, starting with the roughest, I polished the light guide until it was clear. Then, ethyl alcohol was used to clean the light guide. Acetone was used to clean the lens of the PMT.

Next, I made optical cement for the PMT. The brand name of the optical cement used is EJ-500 made by Eljen Technology. The cement consists of the resin and hardener solution. To make the solution, I weighed out 4 grams of the resin and 1 gram of the hardener and mixed them together with a glass rod in a small cup. The mixture was left to sit for 15 minutes to ensure that the cement was clear of air bubbles so that light transmittance is not distorted.

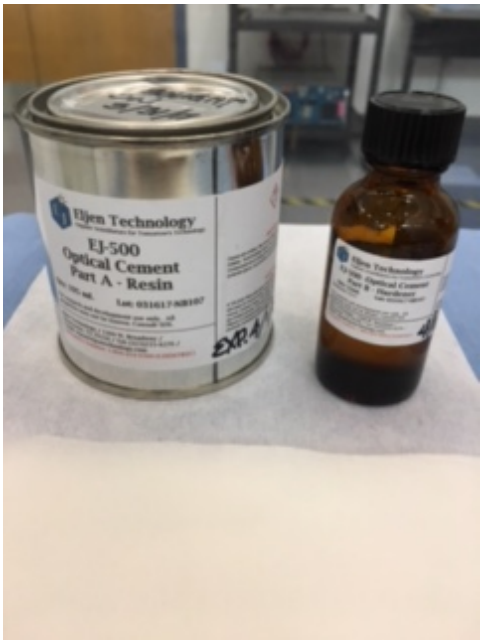

Figure 14 The resin (right) and the hardener (left) for the optical cement

Photo credit: Juan Lukas Rodriguez

While the cement was resting, I taped a thin acrylic sheet around the light guide to help center the PMT. The cement was then applied to the PMT using a glass rod. A quarter-sized amount of cement is placed in the center of the PMT and slowly smoothed out over its surface. With a swift, careful motion, I placed the PMT onto the light guide and held it in place with tape to allow the cement to dry overnight.

3.3. Completing the Replacement Procedure

The next day, with the cement cured, the mu-metal shielding and barrel was placed back over the light guide and secured with the U bolt brace. I re-wrapped the barrel with aluminum and Mylar and secured with black electrical tape. The voltage divider was also re-inserted, taped, and grounded with copper tape to the aluminum foil.

CHAPTER 4

DATA ANALYSIS

4.1. ROOT Graphs

We used a program called ROOT for data analysis. ROOT is a computer program developed by CERN. It is written in C and has many data analysis libraries and functions used for high-energy physics. ROOT is built for data analysis because it can process large amounts of data quickly. I used ROOT to create graphs of the data obtained from data acquisition. The graphs included histograms of the TDC and ADC data.

One histogram from the TDC data was created for each PMT (Figure 15). The graphs show the number of counts for each channel, where each channel equals 50 ps. The TDC histograms in Figure 15 generally show a wide peak for the left PMTs and a narrow peak for the right PMTs. The wide peak for the left PMTs can show us the location of each event. Events that happened close to the left PMT took less time to stop the TDC timing and events that happened further away from the PMT took more time to stop TDC timing. The right PMTs are narrow because they are on the side of the bottom right, which the PMT that starts the TDC timing. The bottom right PMT histogram, however, only shows counts in one channel because the bottom right PMT was delayed in the trigger logic by 31 ns and was the last one to reach the fourfold logic unit which allows the TDC to start counting. And since the bottom right signal is always the one starting the counting it will always have the same amount of time in between the start signal and its TDC stop signal.

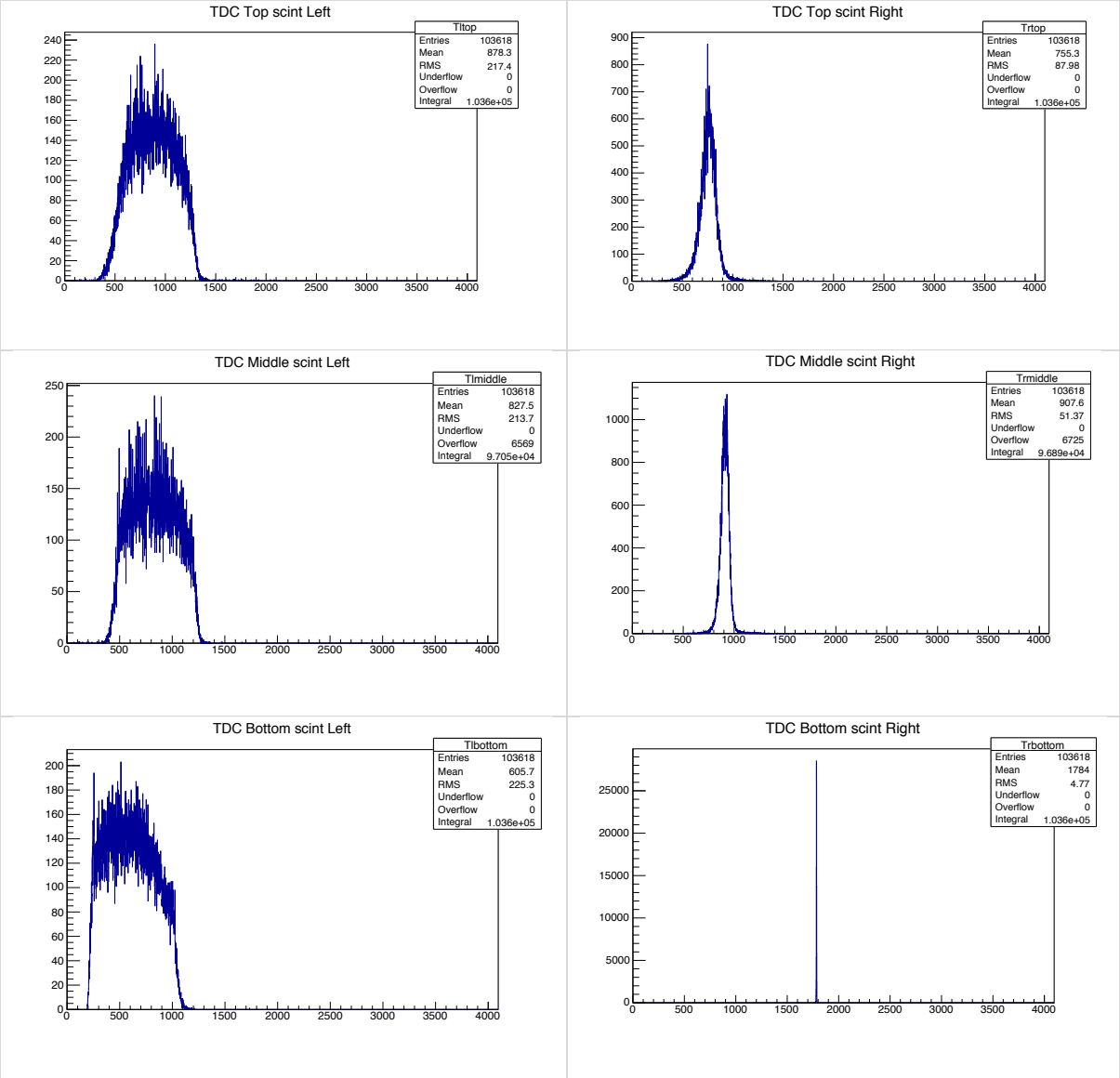

Figure 15 TDC spectra for Scintillators 38 (top), 45 (middle), and 43 (bottom)

These show the number counts (y-axis) for each channel (x-axis). Each channel corresponds to 50 ps.

One ADC graph was also created for each PMT. These show the pulse height (integrated charge) of the signals; see Figure 16 below. The size of the signal is proportional to the energy the particles deposit in the scintillator. The pulse height also

depends on the distance of the event from the PMT and the voltage applied on the PMT. Figure 16 shows a histogram plot of the ADC data. It shows a sharp rise in the beginning followed by a dip and then a second peak. This first sharp rise is noise the PMT generates. The second peak is the actual signal we measure.

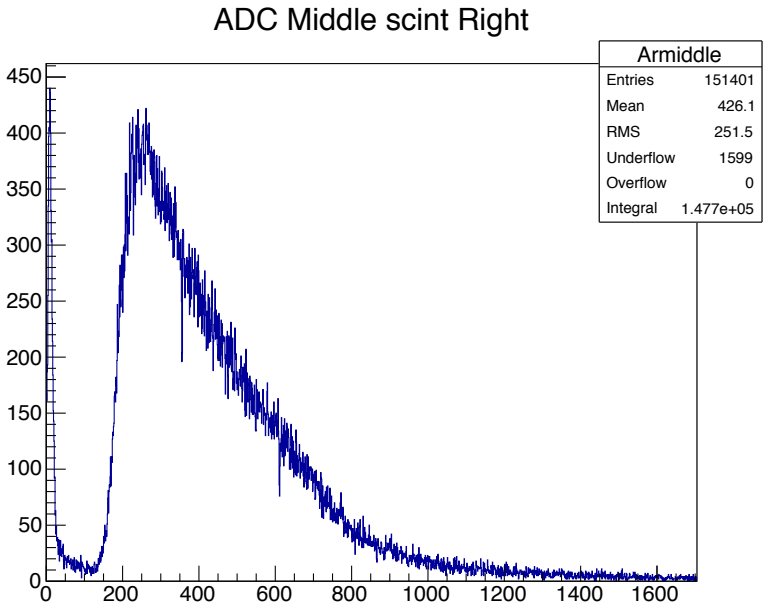

Figure 16 Number of counts vs ADC channel number for the Middle Right PMT

Root also made more advanced graphs using the ADC and TDC data. For example, it created a scatterplot of the ADC left vs the ADC right channel (Figure 19). This shows us the pulse height generated by left PMT vs the right PMT for each event. This will help eliminate noise (see section 4.2). It also created a scatterplot of the TDC difference between the left and right vs the ratio of ADC left and ADC right (Figure 17) . This produces a nice visual of the pulse height in left PMT relative to the right PMT and the location in the scintillator for each event. This shows that the event location affects

the pulse height. When an event is close to a PMT, the pulse height generated is greater. This graph will help us calculate attention length later in this chapter.

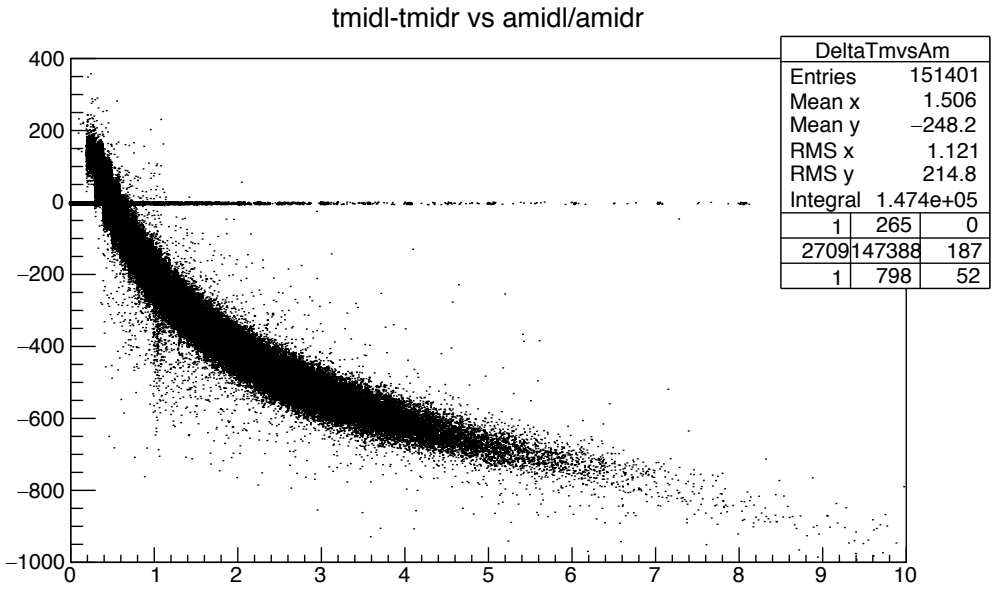

Figure 17 TDC Difference vs ADC Ratio

X-axis is ADC left / ADC right; Y-axis is TDC left – TDC right

4.2. Efficiency

Efficiency is the probability that the middle Scintillator registers an event. It equals the number of events detected by the middle scintillator divided by the total number of triggers. The readings of the TDC graphs of each individual PMT allow the efficiency to be calculated. I looked at the number of events the testing scintillator missed that the trigger scintillators observed. Overflow occurs when the TDC starts but has no stop. If there is no stop, it means there was no signal in the testing scintillator PMT. I calculated efficiency by taking one minus the overflow divided by the total

number of entries. In Figure 15, the overflow number in the top right corner of the graph shows the number of events the middle scintillator missed that the top and bottom scintillators triggered. To cut out some noise in the TDC histograms, the top and bottom ADC left vs ADC right graph was evaluated as described in the next paragraph (see Figure 19). Increasing the voltage in the PMT, increases the efficiency. In Figure 18, you can see the efficiency increase with voltage and then level out once it reaches around 95%. Every PMT reached a range of approximately 94% - 96% efficiency (see table 1 in Chapter 5).

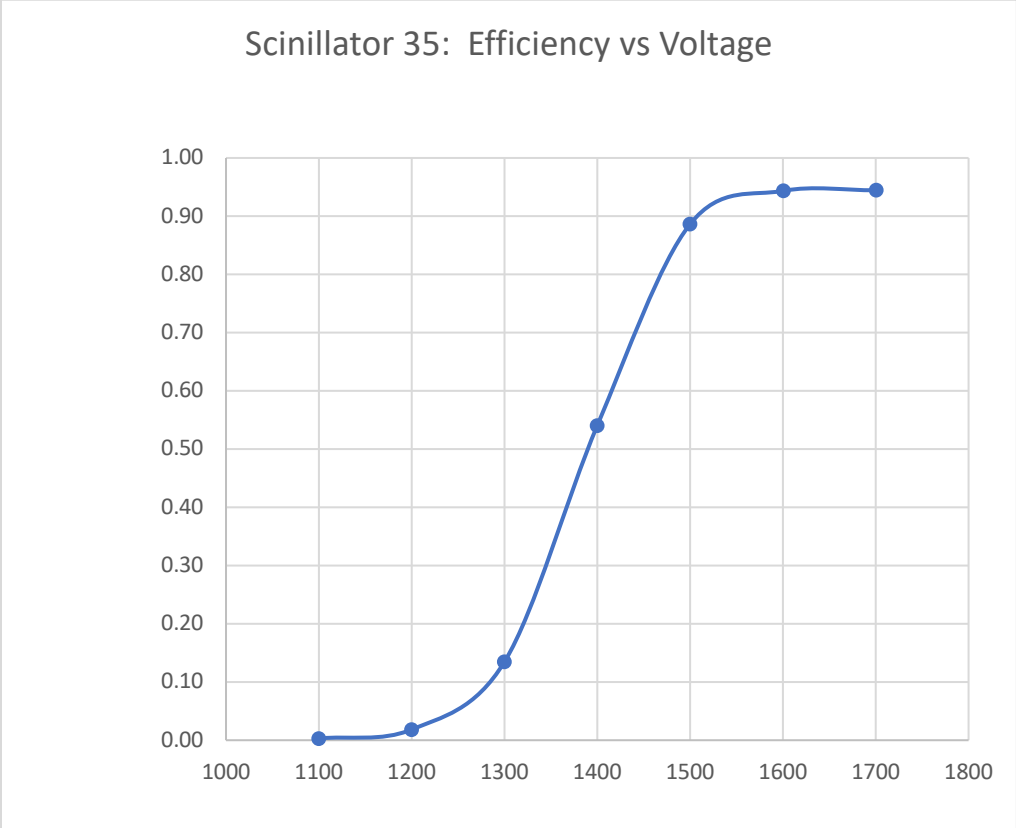

Figure 18 Scatter plot for Efficiency vs Voltage

The x-axis is voltage and the y-axis is efficiency.

Efficiency of the scintillators is better measured when noise is eliminated. The scatter plot below shows the ADC spectra or pulse height in the top left PMT versus that of the top right PMT. Most good signals occurred above and to the right of the greenish curved area. The points in the lower left corner, below and left of the green curved area, are predominantly due to PMT noise. This noise is eliminated by not including in our analysis those events.

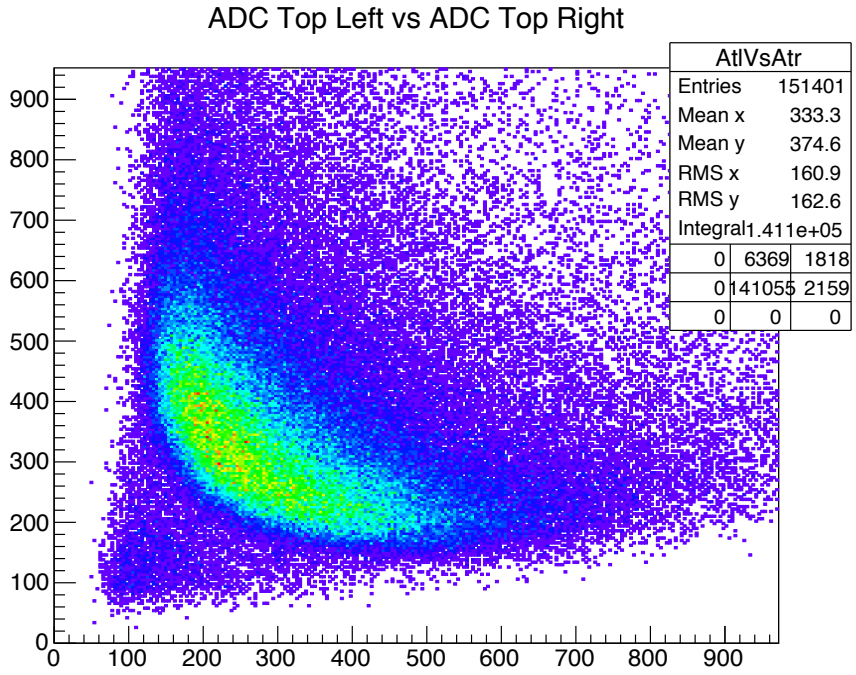

Figure 19 ADC Top Left vs ADC Top Right

The noise on the bottom left outside of the curve was eliminated to attain a more precise efficiency. The greener the color, the greater the density of the spectra hits.

4.3. Pulse Height

The ADC measures the pulse height of the signals generated by the PMT. This corresponds to the amount of charge the PMT generates for each signal. This depends on

the voltage applied to the PMT and the amount of energy the particles deposit on the scintillators.

To measure the pulse height, we looked at the channel where the ADC peaked. We usually aimed for the ADC peak to be at least 250 channels. When the pulse height peaks were less than 250 channels, we increased the voltage in order to raise the pulse height. Figures 20 and 21 show the pulse height increasing when increased voltage was applied to the right PMT from Scintillator 45. When voltage gets too high, the graph begins to flatten out (Figure 21). This shows a PMT with inconsistent signals which can be corrected by lowering the voltage.

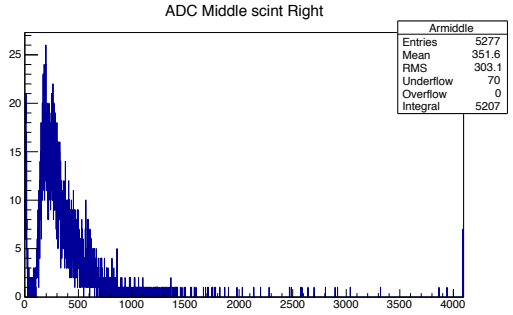

Figure 20 Scintillator 45 Right PMT at 1600 V

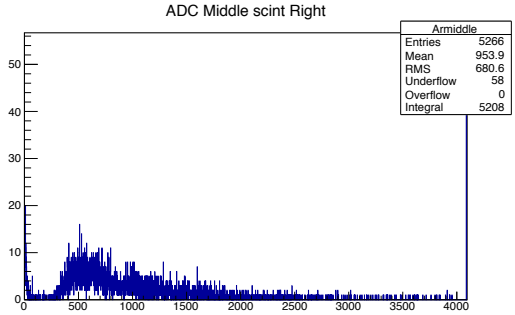

Figure 21 Scintillator 45 Right PMT at 1800 V

4.4. Light Attenuation

When charged particles enter the scintillator, the atoms of the scintillator material excite and then produce a flash of light. This light then travels through the scintillator to the light guide. During this travel, the light gradually loses intensity because some photons interact with the atoms of the scintillator. This decrease in intensity is known as attenuation. The loss in intensity as a function of distance is described by:

$$\text{Eq 1:} \quad I(x) = I_0 e^{-\mu x}$$

Where I_0 is the incident beam intensity, μ is the absorption coefficient, and x is the distance the beam travels.

One of the tasks for this project was to calculate the attenuation length, which is the distance that decreases the intensity of the light to 1/e, or by about 63%. The attenuation length is related to the inverse of the absorption coefficient μ in equation 1. I used equation 1 to derive an equation for each PMT's ADC signal: $A_L = Ce^{-x/d}$ *and* $A_R = C'e^{-(L-x)/d}$ where A_L and A_R are the ADC signal for the left and right PMT, C and C' are constants, L is the length of the scintillator, and d is the attenuation length. Dividing A_L by A_R and absorbing all the constants in C" we get:

$$\text{Eq 2:} \quad \frac{A_L}{A_R} = C''e^{-2x/d}$$

The graph in Figure 22 shows the scatter plot of the TDC difference versus the natural log of the ADC ratio which is used to derive equation 3. Equation 3 is the y-intercept formula of the decreasing slope of the diagonal line defined by the greatest density of the data pattern (bright green color on the graph). The Δt is the y-axis, a is a constant, b is the slope; and the natural log of the ADC channel is the x-axis.

$$\text{Eq 3:} \quad \Delta t = a + b * ln(\frac{A_L}{A_R})$$

Using $x = v\,\Delta t$ and solving for the ADC ratio we get:

$$\text{Eq 4:} \quad \frac{A_L}{A_R} = e^{\frac{2x-L}{bv}}$$

Next, we equate equation 4 and equation 2 and solve for the attenuation length d:

$$\text{Eq 5:} \quad d = -bv$$

Thus, the attenuation length depends on the slope of data line and the velocity of the photons traveling through the scintillator. Velocity shown here in equation 6:

$$\text{Eq 6: } v = \frac{2L}{\Delta tmax - \Delta tmin}$$

Where $\Delta tmax$ is the max time difference and $\Delta tmin$ is the minimum time difference show on the y-axis of Figure 22. The attenuation lengths are tabulated in Table 2.

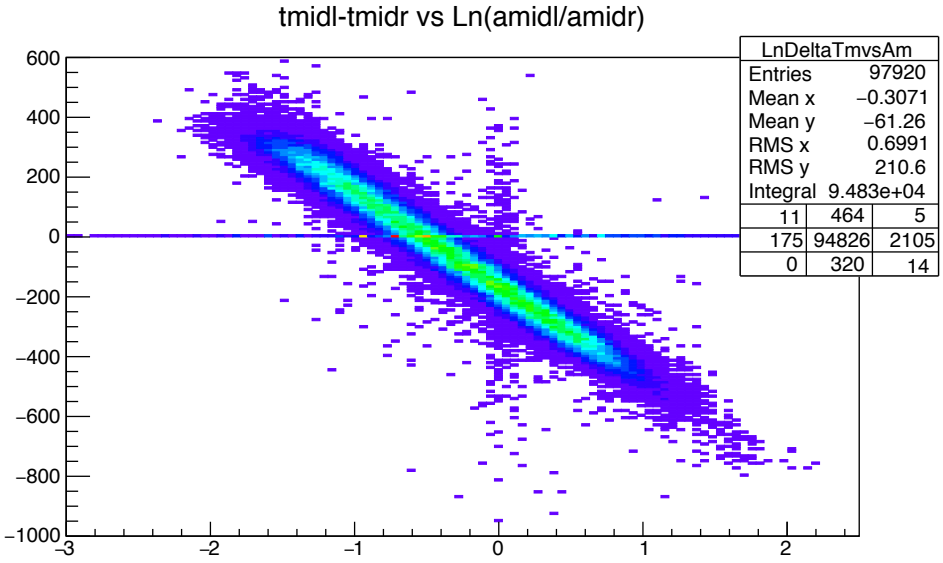

Figure 22 Scatter plot of TDC vs Natural Log

On the x-axis is the natural log of the ratio of the left and right ADC channel ($\ln(\frac{A_L}{A_R})$). On the y-axis is the TDC channel difference between the left and the right, which is the time difference (Δt).

4.5. Time Resolution

Time resolution of a scintillator detector is how precisely we can measure the time of flight of an incident particle. The time it takes the particle to travel through the PMTs is related to the distance it must travel and the shape of the materials it is passing through. To measure time resolution, a histogram (Figure 23) is plotted using the equation:

Eq: *(Tl + Tr + Bl + Br)/4 – (Ml + Mr)/2 = Tdiff*

Where *Tl* and *Tr* are the top left and right TDC channel, *Bl* and *Br* are the bottom left and right TDC channel, and *Ml* and *Mr* are the middle left and right TDC channel. This equation shows us the time a cosmic ray passes through the middle scintillator relative to the two reference scintillators. A Gaussian curve is then fitted to the histogram to find the sigma value in channels. Once the sigma value is found it is multiplied by 50 pico seconds to calculate time resolution. See chapter 5 for the time resolution for each scintillator.

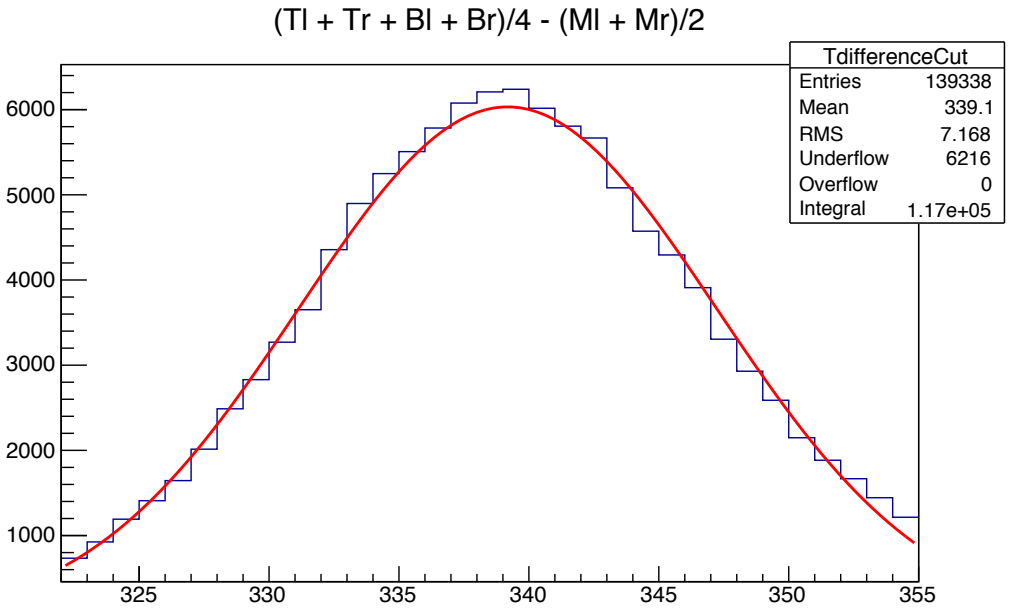

Figure 23 Histogram of Time Resolution for Scintillator 38

2350 V left and 2400 V right with Gausian fit. X-axis is Time Resolution; y-axis is counts.

CHAPTER 5

RESULTS

All eleven scintillators and 22 PMTs were measured for efficiency, pulse height, time resolution, and light attenuation. The results of the testing for Scintillators 35- 45 and their PMTs are shown in tables in this chapter.

Table 2 Optimal Voltages for PMTs in Scintillators 35-45

PMT	Optimal Voltage	Efficiency	Pulse Height (channel)
45L	1750v	94.88% ± .07%	234
45R	1650v	94.72% ± .07%	281
44L	1800v	95.33% ± .03%	230
44R	1800v	95.79% ± .03%	600
43L (new 1160)	1600v	93.48% ± .04%	190
43R	1600v	94.45% ± .04%	250
42L	1950v	95.82% ± .06%	240
42R	1600v	95.68% ± .06%	470
41L (new 1162)	1400v	94.75% ± .06%	253
41R (new 1161)	1500v	94.57% ± .06%	241
40L (new 1164)	1450v	95.17% ± .06%	259
40R	1750v	95.08% ± .06%	265
39L	2350v	95.56% ± .03%	260
39R (new 1158)	1350v	95.52% ± .04%	400
38L	2350v	95.37% ± .05%	250
38R	2400v	95.16% ± .05%	246
37L	2400v	94.41% ± .08%	209
37R	2200v	94.53% ± .07%	266
36L	1850v	95.12% ± .07%	235
36R	2250v	95.19% ± .06%	218
35L (new 1166)	1650v	95.40% ± .05%	306
35R (new 1165)	1450v	95.15% ± .05%	257

After completing voltage tests and analyzing the data, I determined optimal voltage by selecting the highest efficiency and the pulse height with at least 250 in ADC channel values. Optimal voltage, efficiency, and pulse height values for each PMT are shown in Table 2. Of the 22 PMTs I tested, seven were replaced (39R, 43L, 41R, 41L, 40L, 35R, and 35L) and their new PMT numbers are shown in the table. Optimal voltages ranged from 1350 V to 2400 V; efficiency values ranged from 94% to 96%; and the pulse heights ranged from 190 channels to 470 channels. The efficiency is less than 100% due to geometrical effects.

Light attenuation and Time Resolution values for Scintillators 35-45 were also recorded in Table 3 below.

Table 3 Light Attenuation and Time Resolution for Scintillators 35-45

Scintillator	Attenuation (meters)	Time resolution (pico seconds)
45	3.2 ± .3	400 ± 10
44	3.0 ± .3	425 ± 15
43	3.6 ± .3	500 ± 10
42	3.7 ± .3	525 ± 15
41	4.0 ± .3	385 ± 15
40	3.6 ± .3	390 ± 15
39	3.4 ± .3	390 ± 15
38	4.4 ± .3	390 ± 15
37	4.7 ± .3	450 ± 15
36	3.8 ± .3	575 ± 15
35	4.0 ± .3	403 ±15

For Scintillators 35-45, the attenuation lengths as measured ranged from 3.0 to 4.7 meters. The uncertainty for the attenuation length come from the uncertainty in calculation the slope as well as the time difference values in Figure 22. These are appropriate lengths compared to JLab data where the attenuation length for scintillator model BC-408 was found to be 3.8 meters.[6] These lengths are also around the lengths of the scintillators which is generally what we want the attenuation length to be. The time resolution values ranged from 390 pico seconds to 575 pico seconds. The time resolution values show us the error in calculating time of flight of an incident particle.

[6] https://halldweb.jlab.org/wiki/images/b/b1/Scintillators.pdf

CHAPTER 6

CONCLUSION

Testing and refurbishing the scintillators and PMTs sent from JLab's Hall B to ODU's High Bay Lab were important steps in prolonging the effectiveness of the equipment and preparing them for reuse in future experiments. Of the 22 PMTs I tested, I removed and replaced 7 PMTs. From testing, I discovered the optimal voltages to achieve appropriate efficiency and pulse height. All eleven scintillators were refurbished and I calculated attenuation length and time resolution.

These eleven scintillators were sent back to Jefferson Lab in June 2017. They will be used in the EMC-SRC experiment in Hall C. The next and final frame of scintillators from JLab are currently being tested and refurbished at ODU. They are scheduled to return to JLab in August 2017.

BIBLIOGRAPHY

[1] Jefferson Laboratory websites: https://www.jlab.org; and https://halldweb.jlab.org/wiki/images/b/b1/Scintillators.pdf

[2] Leo, W.R. *Techniques for Nuclear and Particle Physics Experiments: A How-To Approach*. New York: Springer-Verlag, 1994.

[3] McArthur, Korac J. *UNH Nuclear Instrumentation Lab CEBAF Time of Flight Detectors Final Project Report*, July 17, 1996. Jefferson Laboratory website library.

[4] McMahan, Katheryne. *Scintillator Testing and Repair for the Large Acceptance Detector at Jefferson Lab*. Norfolk: Old Dominion University, December 2015.

[5] Saunders, Noel. *JLab Particle Detectors, Used in Nuclear Research, Arrive for Refurbishment*. June 2017. Old Dominion University website: https://www.odu.edu/news/2017/6/particle_detector#.WWuu5Iokqt8

[6] Smith, E.S., et al. *The Time-of-Flight System for CLAS*. NH Elsevier: Nuclear Instruments and Methods in Physics Research A 432 (1999) 265-298.